Convergence in the temperature response of leaf respiration across biomes and plant functional types

Mary A. Heskel[a,b], Odhran S. O'Sullivan[a,c], Peter B. Reich[d,e], Mark G. Tjoelker[d], Lasantha K. Weerasinghe[a,f], Aurore Penillard[a], John J. G. Egerton[a], Danielle Creek[a,d], Keith J. Bloomfield[a], Jen Xiang[g], Felipe Sinca[h], Zsofia R. Stangl[i], Alberto Martinez-de la Torre[j], Kevin L. Griffin[k,l], Chris Huntingford[j], Vaughan Hurry[m], Patrick Meir[a,n], Matthew H. Turnbull[o], and Owen K. Atkin[a,g,1]

[a]Division of Plant Sciences, Research School of Biology, The Australian National University, Canberra, ACT 2601, Australia; [b]The Ecosystems Center, Marine Biological Laboratory, Woods Hole, MA 02543; [c]Animal and Plant Sciences, The University of Sheffield, Sheffield, S10 2TN United Kingdom; [d]Hawkesbury Institute for the Environment, Western Sydney University, Penrith, NSW 2751, Australia; [e]Department of Forest Resources, University of Minnesota, St. Paul, MN 55108; [f]Faculty of Agriculture, University of Peradeniya, Peradeniya, 20400 Sri Lanka; [g]ARC Centre of Excellence in Plant Energy Biology, Research School of Biology, The Australian National University, Canberra, ACT 2601, Australia; [h]Department of Global Ecology, Carnegie Institution for Science, Stanford University, CA 94305; [i]Umeå Plant Science Centre, Department of Plant Physiology, Umeå University, SE-901 87 Umea, Sweden; [j]Biosphere-Atmosphere Interactions, Centre for Ecology and Hydrology, Wallingford OX10 8BB, United Kingdom; [k]Department of Earth and Environment Sciences, Columbia University, Palisades, NY 10964; [l]Department of Ecology, Evolution, and Environmental Biology, Columbia University, New York, NY 10027; [m]Umeå Plant Science Centre, Department of Forest Genetics and Plant Physiology, Swedish University of Agricultural Sciences, SE-901 83 Umeå, Sweden; [n]School of Geosciences, University of Edinburgh, Edinburgh EH8 9XP, United Kingdom; and [o]Centre for Integrative Ecology, School of Biological Sciences, University of Canterbury, Christchurch, 8140, New Zealand

Plant respiration constitutes a massive carbon flux to the atmosphere, and a major control on the evolution of the global carbon cycle. It therefore has the potential to modulate levels of climate change due to the human burning of fossil fuels. Neither current physiological nor terrestrial biosphere models adequately describe its short-term temperature response, and even minor differences in the shape of the response curve can significantly impact estimates of ecosystem carbon release and/or storage. Given this, it is critical to establish whether there are predictable patterns in the shape of the respiration–temperature response curve, and thus in the intrinsic temperature sensitivity of respiration across the globe. Analyzing measurements in a comprehensive database for 231 species spanning 7 biomes, we demonstrate that temperature-dependent increases in leaf respiration do not follow a commonly used exponential function. Instead, we find a decelerating function as leaves warm, reflecting a declining sensitivity to higher temperatures that is remarkably uniform across all biomes and plant functional types. Such convergence in the temperature sensitivity of leaf respiration suggests that there are universally applicable controls on the temperature response of plant energy metabolism, such that a single new function can predict the temperature dependence of leaf respiration for global vegetation. This simple function enables straightforward description of plant respiration in the land-surface components of coupled earth system models. Our cross-biome analyses shows significant implications for such fluxes in cold climates, generally projecting lower values compared with previous estimates.

temperature sensitivity | climate models | carbon exchange | Q_{10} | thermal response

Plant respiration provides continuous metabolic support for growth and maintenance of all tissues and contributes ~60 Pg C y^{-1} to the atmosphere (1, 2), with ~50% of the carbon (C) released by whole-plant respiration from leaves (3). As rates of leaf respiration (R) vary substantially with changes in temperature (T) (4, 5), even slight increases in ambient T can lead to increases in the flux of carbon dioxide (CO_2) from leaves to the atmosphere. This has the potential to create concomitant decreases in net primary productivity, and affect the implications of fossil fuel burning by contributing additionally to atmospheric CO_2 levels due to any imposed surface-level global warming. Hence, quantification of the T response of leaf R, and how this response may vary across diverse ecosystems and plant species, is critical to current estimations and future projections of the global carbon cycle (6–8). Evaluating how leaf R relates to T in terrestrial plants will clarify fundamental controls on energy metabolism and enable more accurate parameterization, as leaf R, in addition to photosynthesis (9, 10), has been

identified as a major source of uncertainty in models of the global carbon cycle (8, 11). The response of leaf R to T differs in both magnitude and mechanism with time scale (5); herein, we address how the fundamental short-term response (minutes to hours) varies among plant species and biomes globally.

The short-term T response of leaf R is strongly regulated by the T dependence of the reaction rates of enzymes involved in a variety of respiratory pathways in the cytosol and mitochondria within plant cells (5, 12). Given that these many processes influence the realized rates of leaf R across broad ranges in T, the T dependence of R might be expected to vary widely among contrasting thermal regimes and environments, or among species that differ in metabolic capacity or life span. For example, R–T relations could vary predictably, according to plant functional types (PFTs; groupings of plant species by life history attributes, growth strategies and/or geographic location), or with variation corresponding with types that differ in rates of net photosynthetic CO_2 uptake and potential growth rates (e.g., fast-growing herbs

Significance

A major concern for terrestrial biosphere models is accounting for the temperature response of leaf respiration at regional/global scales. Most biosphere models incorrectly assume that respiration increases exponentially with rising temperature, with profound effects for predicted ecosystem carbon exchange. Based on a study of 231 species in 7 biomes, we find that the rise in respiration with temperature can be generalized across biomes and plant types, with temperature sensitivity declining as leaves warm. This finding indicates universally conserved controls on the temperature sensitivity of leaf metabolism. Accounting for the temperature function markedly lowers simulated respiration rates in cold biomes, which has important consequences for estimates of carbon storage in vegetation, predicted concentrations of atmospheric carbon dioxide, and future surface temperatures.

versus slower-growing trees). A key issue, therefore, is whether the *T* dependence of leaf *R* has spatially invariant features across the earth's surface, or instead varies as a consequence of genotypic and multiple environmental factors. This is critically important, as the global estimation of leaf *R* is a significant uncertainty in terrestrial biosphere models (TBMs) and associated land-surface components of earth system models (ESMs). The latter quantify the global carbon cycle now and project it into the future (8, 11), including feedbacks as a consequence of anthropogenic emissions of CO_2 on climate.

Although it has been known for over a century that the near-instantaneous increase in plant *R* with rising *T* is nonlinear (13, 14), there has been uncertainty whether a single general form for the leaf *R*–*T* relationship applies both phylogenetically and biogeographically (15–17). A widely adopted physiological model framework (18, 19) assumes that *R* exhibits an exponential response to *T*, with *R* roughly doubling with every 10 °C rise in *T* (corresponding to a fixed "Q_{10}-type" formulation, with $Q_{10} \sim$ 2.0). However, it has long been recognized that the Q_{10} is often not constant nor close to 2.0 except over a limited *T* range (14, 20), and this pattern is consistent when also considering ecosystem respiration (21). For this reason, alternative models have been developed, including modified Arrhenius formulations, universal temperature dependence (UTD), and *T*-dependent Q_{10} functions (15–17, 22). All of these models attempt to address the shortcomings of an exponential model that provides a fixed *T*-sensitivity term across a wide range of temperatures. Here, we evaluate a comprehensive set of empirical, thermally high-resolution *T*-response curves for multiple taxa and environments. Doing so enables a full assessment of the suitability of these quantitative physiological models in accurately representing the variation in the observed short-term *R*–*T* relationship, and implications of the short-term response in different seasons. We aim to significantly improve how the short-term *R*–*T* response is represented, and recognize this is one element of a complex and dynamic process. As leaf *R* is also impacted by acclimation to sustained changes in growth *T*, future modeling work will determine the effect of a more accurate short-term *T* response applied in concert with recent advances in modeling basal rates of leaf *R* (23) and longer-term (weeks to months) acclimation of *R* to changing growth *T*s (24, 25).

Physiological model representations of leaf respiratory *T* responses vary in complexity and in their ability to account for observed biological patterns, such as decreases in the *T* sensitivity of *R* over increasing *T*s (5, 17) (see *Supporting Information* for model descriptions and Figs. S1 and S2). Modification of the *T* sensitivity of leaf *R* (based on ref. 16) in TBMs and the associated land-surface component of ESMs results in significant alterations to modeled carbon fluxes (8, 26), demonstrating the high sensitivity of the carbon cycle simulations to the *R*–*T* function, and thus the need to improve our understanding and quantification of this relationship. The evidence for apparent complexity in the leaf *R*–*T* response (16, 27) and consequences for carbon cycling indicates both the need for, and, opportunity to improve quantification of the leaf *R*–*T* relationship in globally widespread, but thermally contrasting, biomes. Here, we report on filling that critical knowledge gap.

The goals of our study are threefold: (*i*) to quantify the *T* response of leaf *R* through use of a new and comprehensive set of thermally high-resolution field measurements of leaf *R* across large *T* ranges for each leaf; (*ii*) to assess the shape of *T*-response curves in leaves of species representing diverse environments and PFTs; and (*iii*) to assess the implications of altered *T* sensitivity of *R* for simulated carbon fluxes using the land-surface component of a leading ESM (28). Using methods (27) that enabled high-resolution measurement of the *T* dependence of leaf *R* in leaves, we present results from 673 short-term *T*-response curves of 231 species collected in situ across 18 sites representing contrasting biomes, geographical

locations, and PFTs (Table S1). Based on this unprecedented dataset of standardized physiological measurements, we provide evidence of a global, fundamental *T* response of leaf *R* in terrestrial plants and thus a mathematical model that outperforms alternative representations of how leaf *R* responds to *T*. We also show that in cross-biome analyses, application of this mathematical model significantly alters simulated carbon fluxes, particularly in cold climate ecosystems.

Results

Evaluating Temperature Response Models. Our data of high-resolution measurement of the *T* response of leaf *R* enabled a comparison of commonly applied quantitative physiological models to determine which offered the best fit for replicate response curves across the entire 10–45 °C range. A comparison of residuals from model estimates for all individual leaf response curves for five models (exponential fixed-Q_{10}, Arrhenius, Lloyd & Taylor, variable-Q_{10}, and second-order log-polynomial function; *Supporting Information*) demonstrates that a second-order log-polynomial model best characterized the *T* response of *R* (Fig. S2A). This selection is made on the basis that the polynomial model had the best projections of leaf *R* against data from over the entire *T* range, has a straightforward application, and is independent from biological assumptions about activation energies; we applied this approach to all measured response curves that collectively comprise the total mean response (Fig. S2B). Accordingly, to best represent our high-resolution leaf *R* measurements quantitatively, all individual leaf *T*-response curve data were natural-log–transformed (*ln*) and to those values, a second-order polynomial model was fitted as:

$$ln\,R = a + bT + cT^2, \qquad [1]$$

where *R* is the rate at a given leaf *T*, and *a*, *b*, and *c* are coefficients that provided the fit that minimized residuals.

The application of a polynomial model fit to high-resolution *ln R*–*T* response curves provides a three-parameter description of leaf *R* across the *T* range. The *a* parameter, which indicates *ln R* at 0 °C, determines a reference value offset of the response curve. The *b* parameter—the slope of *ln R* vs. *T* plot at 0 °C—and the *c* parameter, which represents any quadratic nonlinearity in *ln R* vs. *T* slope with increasing measuring *T*, are both key to describing the fundamental shape of the short-term *T* response of leaf *R*. To assess the influence of site environment and plant form, we analyzed the variation in values of each model parameter, *a*, *b*, and *c* for diverse biomes and PFTs based on individual leaf sample curves. We calculated this variation for both the entire measured *T* range (10–45 °C), as well as for shorter, discrete segments (i.e., 15–25 °C) of the entire measured *T* range, to evaluate potential influence of measurement *T* range on these parameters. No difference was found between the parameters calculated from shorter, discrete *T* ranges and the entire measurement *T* range, (Tables S2 and S3, Fig. S3), further justifying the applicability of the polynomial function for this response. Together, mean values of *a*, *b*, and *c* parameters create data-derived equations for leaf *R* that clearly mirror observed mean respiratory responses aggregated for discrete levels of the two corresponding factors (i.e., biome or PFT; Fig. 1). This approach can also fully capture the deceleration of rates of *R* observed as *T*s increase (Figs. 1 and S1), clearly demonstrating the utility of the polynomial formulation for creating realistic models of leaf *R*.

Comparison Among Biomes and Plant Functional Types. Mean species values for the polynomial model parameters (*a*, *b*, and *c*) at each site were statistically compared by biome and PFTs using a nested mixed-model approach (Table 1). The curves presented in Fig. 1 show that rates of leaf *R* at a common *T* were highest in the coldest biomes (i.e., higher *a* values for tundra and high-altitude
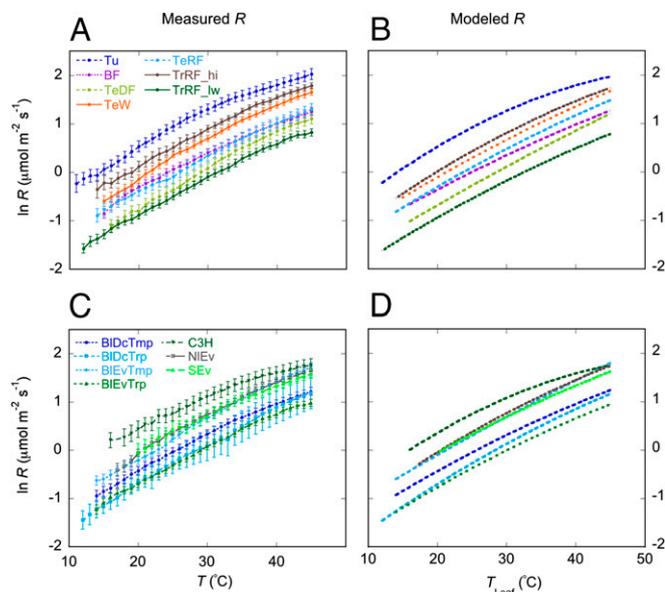
Fig. 1. Mean measured leaf respiration (natural log transformed; ±SE) of biome (*A*) and PFTs (*C*) calculated for each degree Centigrade from measured species respiration response curves of those categories, for the available temperature ranges. Polynomial models based on species' mean values of *a*, *b*, and *c* (Table 1) of those biomes (*B*) and PFTs (*D*) are shown across the same *T* range.

tropical rainforests). By contrast, low-altitude tropical forests, the warmest biome included in this study (Table S1), exhibited the lowest value of parameter *a* and the lowest values of leaf *R* over the measurement ranges of *T* (Fig. 1 *A* and *B*). Similarly,

variation in leaf *R* at a common *T* was found among PFTs (Fig. 1 *C* and *D*).

In strong contrast to large differences across biomes and PFTs in leaf *R* at a common measurement *T*, we found that the rise in *R* with *T* as leaves warm follows a remarkably consistent function, suggesting more universal values of parameters *b* and *c*. Fig. 1 illustrates the common shape of the response curve to leaf *T* that is almost invariant across plants, despite representing highly diverse growth environments and functional groups. This low variation across species means of both *b* and *c* parameters is present when grouped by either biome or PFT (Table 1).

Based on our observation of a near-universal shared response shape of leaf *R* to *T*, we determined the parameters for our global polynomial *R*–*T* model (GPM) of Eq. **1**. The mean polynomial model parameter values for all species included in our study were: *b* = 0.1012 and *c* = −0.0005, which generate the GPM:

$$ln\,R = a + 0.1012T - 0.0005T^2, \qquad \textbf{[2]}$$

where *ln R* and *a* are as defined for Eq. **1**. This equation is an empirically based mathematical model of the instantaneous *T* response of leaf *R* (Fig. 2*A*). Average leaf *R* for all study species across the 10–45° *T* range (within 1 °C temperature bins; untransformed global mean response in Fig. S2*B*)—the "global mean data"—can be effectively summarized by the GPM (Fig. 2*A*). Values of *a* do, however, vary significantly across PFTs, shifting the curve of Eq. 2; thus, the *a* parameter value should be appropriately assigned in the GPM to fit the model's application, using a rate measured at a known *T* or values from our global survey (Dataset S1).

The input of a known value of leaf *R* ($R_{T_{ref}}$ in the below equation), measured at a *T* (T_{ref} in the below equation) with the universal *b* and *c* response curve parameters can be applied to a

Table 1. Biome and PFT mean values (with 95% confidence intervals, CI) of *a*, *b*, and *c* coefficients aggregated across all species (*n* = 231)

Biome/PFT	*a*	95% CI	*b*	95% CI	*c*	95% CI
Biome						
Tu	−1.6043[a]	[-1.8372, -1.3713]	0.1277[a]	[0.1190, 0.1364]	−0.00107[a]	[-0.0012, -0.0009]
BF	−2.0043[a]	[-2.2781, -1.7305]	0.0894[a]	[0.0665, 0.1122]	−0.00037[a]	[-0.0008, 0.00003]
TeDF	−2.4286[a]	[-2.7959, -2.0612]	0.0923[a]	[0.0757, 0.1089]	−0.00026[a]	[-0.0006, 0.00004]
TeW	−1.8958[a]	[-2.3435, -1.4481]	0.0974[a]	[0.0716, 0.1232]	−0.00040[a]	[-0.0008, -0.00002]
TeRF	−2.1544[a]	[-2.4057, -1.9032]	0.1014[a]	[0.0773, 0.1255]	−0.00046[a]	[-0.0008, -0.0001]
TrRF_hi	−2.0173[a]	[-2.5325, -1.5021]	0.1154[a]	[0.0956, 0.1352]	−0.00071[a]	[-0.0010, -0.0004]
TrRF_lw	−2.7493[a]	[-2.9831, -2.5155]	0.0998[a]	[0.0879, 0.1117]	−0.00047[a]	[-0.0007, -0.0003]
PFT						
BlDcTmp	−2.2264[ab]	[-2.4829, -1.9699]	0.0993[a]	[0.0829, 0.1158]	−0.00050[a]	[-0.0008, -0.0002]
BlDcTrp	−2.7270[ab]	[-3.6757, -1.7782]	0.1125[a]	[0.0961, 0.1288]	−0.00058[a]	[-0.0008, -0.0003]
BlEvTmp	−1.8106[a]	[-2.3349, -1.2864]	0.0896[a]	[0.0577, 0.1215]	−0.00021[a]	[-0.0007, 0.0003]
BlEvTrp	−2.6105[b]	[-2.8366, -2.3844]	0.1022[a]	[0.0912, 0.1132]	−0.00052[a]	[-0.0007, -0.0003]
C₃H	−1.7507[ab]	[-2.0680, -1.4334]	0.1271[a]	[0.1169, 0.1374]	−0.00110[a]	[-0.0013, -0.0009]
NlEv	−2.0464[ab]	[-2.5569, -1.5358]	0.1125[a]	[0.0934, 0.1316]	−0.00063[a]	[-0.0009, -0.0004]
Sev	−1.8150[a]	[-2.4609, -1.1691]	0.0971[a]	[0.0593, 0.1349]	−0.00047[a]	[-0.0006, -0.0004]
Global mean	−2.2276	[-2.3966, -2.0586]	0.1012	[0.0921, 0.1104]	−0.00050	[-0.0006, -0.0004]

Biomes include tundra (Tu; *n* = 20), boreal forest (BF; *n* = 25), temperate deciduous forest (TeDF; *n* = 10), temperate woodland (TeW; *n* = 67), temperate rainforest (TeRF; *n* = 12), high-elevation tropical rainforest (TrRF_hi; *n* = 16), and low-elevation tropical rainforest (TrRF_lw; *n* = 81); PFTs include broadleaf deciduous temperate (BlDcTmp; *n* = 40), broadleaf deciduous tropical (BlDcTrp; *n* = 4), broadleaf evergreen temperate (BlEvTmp; *n* = 38), broadleaf evergreen tropical (BlEvTrp; *n* = 88), C₃ herbaceous (C₃H; *n* = 13), needle-leaf evergreen (NlEv; *n* = 13), and evergreen shrubs (SEv; *n* = 35). Mean values and confidence intervals were calculated from natural-log–transformed rates of leaf respiration *R*–*T* curve data available from the ~10–45 °C curve range. The global mean value was calculated from all individual species parameter values. To determine the effect Biome and PFT groups, we used a mixed model that nested random effects, with Species nested in Site when evaluating Biome, and Species as a single random effect to evaluate the fixed effect of PFT. Post hoc comparisons of least-square means determined differences between Biome and PFT groups (denoted by unshared letters).
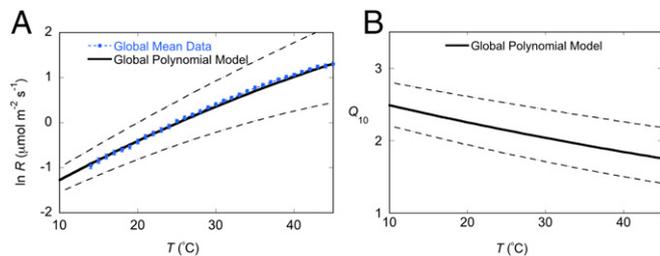
Fig. 2. Global mean data reflected by modeled R–T and corresponding declining Q_{10} responses. The mean T response of (A) natural-log–transformed rates of leaf respiration ($ln R \pm$ SE, Global Mean Data, shown with blue symbols with error bars) for all measured species ($n = 231$) across all biomes and PFTs, overlaid on the GPM of $ln R$ (solid black line, bracketed by dashed lines representing 95% confidence intervals), calculated from the species values of *a, b,* and *c* parameters of the polynomial model. The GPM is defined as $ln R = -2.2276 + 0.1012*T - 0.0005*T^2$. The T response of Q_{10} values (B) based on GPM *b* and *c* coefficients as calculated by $Q_{10} = e^{10*(0.1012+(2*0.0005T))}$, shown with 95% confidence intervals (dashed lines).

derivation of our GPM to predict values of leaf R (R_T) at a desired T, according to:

$$R_T = R_{T_{ref}} \times e^{\left[0.1012 \cdot \left(T - T_{ref} \right) - 0.0005 \cdot \left(T^2 - T_{ref}^2 \right) \right]}, \qquad [3]$$

where $R_{Tref} = \exp\left(a + 0.1012 T_{ref} - 0.0005 T_{ref}^2\right)$. This equation incorporates the common intrinsic T sensitivity of respiration (i.e., response curve shape) observed from our field measurements, and when combined with measured or assumed rates of R at T_{ref}, enables prediction of R at various Ts.

The T sensitivity of the GPM (Fig. 2B), here calculated for illustrative purposes using Q_{10} values, shows decreasing sensitivity of leaf R with increases in T. Up to 35 °C, the decline has similarities to (and a steeper slope than) that reported from more limited data by Tjoelker et al. (16). Moreover, our GPM demonstrates that leaf R remains more T sensitive at higher leaf Ts (e.g., near 45 °C) than assessed by Tjoelker et al. (16).

Impacts on Simulated Annual Respiration. The consequence of using our GPM in existing global models that exclude acclimation responses to sustained changes in growth T is illustrated in Fig. 3, which shows annually averaged rates of leaf R for our 18 field sites, comparing Joint U.K. Land Environmental Simulator (JULES) estimates modeled with a $Q_{10} = 2$ with those from our GPM derivation Eq. 3.

As a sensitivity study, we replaced the derivation of the GPM (Eq. 3) with the commonly applied fixed Q_{10} formulation, setting $Q_{10} = 2$, and compared the two. The difference between annual rates of leaf R calculated using either the derived GPM (Eq. 3) or a fixed Q_{10} equation where $Q_{10} = 2$ had almost no impact on at the warm tropical sites (Fig. 3 *A* and *B*); similarly, there was no effect of the GPM on seasonal variations in leaf R at the tropical sites (Fig. 3C). By contrast, at colder sites, estimates of annual leaf R were markedly lower when calculated using the GPM derivation (e.g., 28% lower in Toolik Lake, Alaska, and 10–20% lower in the temperate sites) compared with the fixed Q_{10} function (Fig. 3B), although recognizing these changes are for generally lower R values. At temperate woodland sites with evergreen, long-lived foliage, replacement of a fixed Q_{10} of 2.0 model with the GPM had its greatest absolute and proportional effect during the cold months of winter, but negligible effect during summer months when leaf T values were near 25 °C. For sites where winters are characterized by winter freezing (and thus where metabolic activity is minimal), use of the GPM reduced estimates of leaf R across the entire growing season (Fig. 3C).

Discussion

Universality of Temperature Response. Despite the huge diversity in plant growth form and local environment represented in our comprehensive dataset, we find remarkable convergence in the functional form of the response of leaf R to T. Basal rates of R vary widely among biomes and PFTs (Fig. 1), and are known to be related to differences in growth T, site aridity, and leaf functional traits (23, 29, 30). That R at a given T is highest in leaves of arctic tundra plants and lowest in leaves of plants from low-elevation tropical forests (Fig. 1A) agrees with the concept that leaf R (when measured at a common T) is higher in plants grown in colder environments (12), and this pattern can be consistently modeled based on known growth Ts (23). There is significant variation in the curve offset between PFTs; C_3 herbs exhibit the highest rates of leaf R across the 10–45 °C range (Fig. 1C), which is also associated with high rates of leaf R at a common leaf nitrogen compared with other PFT groups (23, 29). However, here we show the overall shape of the response curve, and thus intrinsic T sensitivity of R, does not significantly vary;
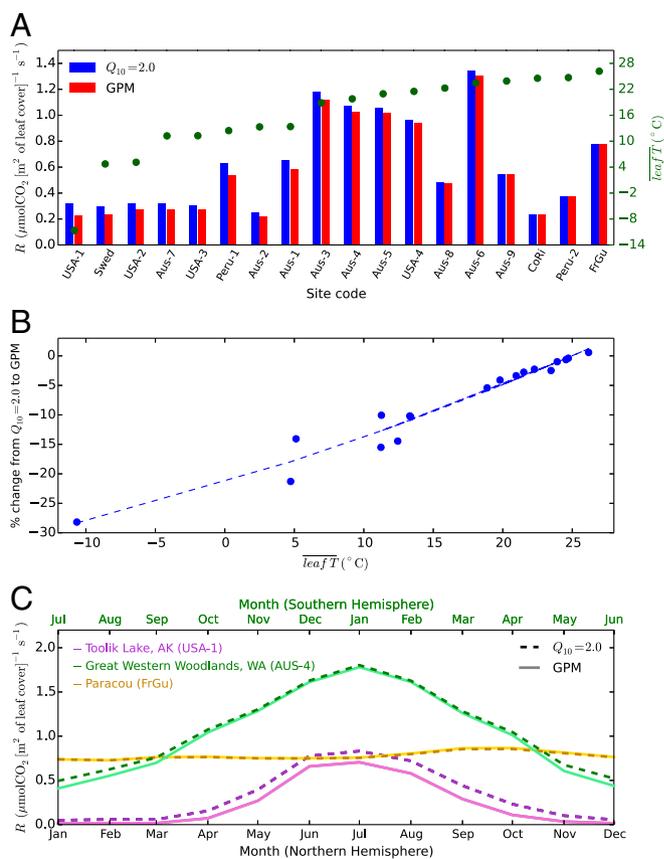

Fig. 3. Impact of two T functions on annual average of modeled instantaneous leaf respiration rates (R) using the JULES coupled climate carbon model to extrapolate respiration measurements (42, 43). *A* shows annual average of leaf R (averaged over the five years of 2010–2014 inclusive) at 18 globally distributed field sites (Table S1), with annual rates of R calculated assuming a fixed Q_{10} of 2.0 (43) or our GPM (Eq. 3). Annual averages of leaf T (same period) in the upper canopy is shown as green dots. Sites are ordered by temperature, with site codes as shown in Table S1; *B* shows percentage changes in annual averages of rates of leaf R that result from switching from a fixed Q_{10} to our GPM, plotted against annual averages of leaf T—the dashed line shows a parabolic curve fit i.e., with three degrees of freedom; *C* shows seasonal variation in rates leaf R (expressed on an LAI basis) for three thermally contrasting sites [Toolik Lake (tundra), Alaska; Great Western Woodlands (temperate woodland), Western Australia; and Paracou (tropical rainforest), French Guiana]. Site-averaged leaf R values at 25 °C, measured in the field, were used for the calculations.

the only variation is an overall offset of the curve. The consistency in the response of leaf R to T strongly suggests its universality among C_3 plants and that the T dependencies of underlying enzymatic controls of multiple metabolic pathways are widely conserved, even among the most thermally contrasting biomes on earth. Further, a global, fundamental T response can be described in a simple, empirically driven log-polynomial equation, available for incorporating into the land-surface component of ESMs and ready to replace current imperfect representations of the short-term T response of leaf R. Notably, when implemented in a leading TBM (28) for different geographical regions, this equation significantly reduces annual rates of leaf-level respiration in cold climates. We believe this global short-term leaf R–T response, when applied in conjunction with data-based models of basal leaf R (23) and the acclimation response to longer-term growth Ts (24), will have important consequences for predicted rates of ecosystem and global carbon exchange, estimates of future carbon storage in vegetation, predicted concentrations of atmospheric CO_2, and impacts of future surface temperatures.

Utility for Predictive Simulation Models. Our finding of a universal T response provides an opportunity for leaf R to be better represented in ecosystem models, TBMs, and associated land-surface components of ESMs. It is well known that the use of a fixed-Q_{10} or Arrhenius activation energy leads to inaccuracies in estimations of respiratory efflux, especially at relatively high and low Ts (5). In particular, Arrhenius-derived functions may overestimate rates at low Ts and underestimate the decline in T sensitivity of R (22) (Fig. S1A). To date, there has been no consensus or consistent assessment based on comprehensive datasets on how to represent the T response of R in simulation models (31). Our GPM (Eq. **1**) and its parameterization (Eqs. **2** and **3**) against a massive dataset for R is comprised of only three and two coefficients, respectively, and offers a simple, yet robust, approach to calculating the T response of R in leaves. Importantly, our GPM demonstrates that leaf R remains T sensitive at high leaf Ts (e.g., near 45 °C; seen in our Fig. S1A compared with variable Q_{10} model; ref. 12), which will have important consequences for predicted rates of respiratory CO_2 efflux at high Ts, particularly as extreme heatwave events are predicted to increase in frequency and duration (2).

Application of the GPM requires knowledge of basal rates of leaf R, designated by the a parameter (Eq. **2**) or measured/assumed rates of R at a standard measurement $T = T_{Ref}$ (Eq. **3**). In cases where the basal rate of R is unknown, we suggest application of specific a parameter values representing appropriate PFTs and/or biomes (Table 1) or species (Dataset S1). Alternatively, rates of leaf R at common T_{Ref} (25 °C) reported in a recent global compilation (23) can be used. We believe future integration of the recent leaf R dataset (23) with the short-term R–T response model defined by our GPM and climatically variable estimates of longer-term T response of R through acclimation will result in a vastly improved representation of leaf R across scales.

Consequences for Terrestrial C Exchange. Our sensitivity study (Fig. 3) showed that although replacing a fixed Q_{10} of 2 with the GPM will have little impact on calculated rates of leaf R in lowland tropical forests, impacts are significant for temperate, boreal, and arctic/alpine ecosystems. In such ecosystems, reliance on a fixed Q_{10} greatly overestimates annual leaf R, which in turn will result in underestimates of net primary productivity (NPP), as generally TBMs estimate NPP by subtraction of total canopy leaf R from modeled estimates of gross primary productivity (GPP). Though future model implementations that consider the extent to which leaf R acclimates to long-term changes in air T across the globe (24, 25) will likely further improve how leaf R is represented in TBMs, our findings point to lower rates of modeled respiratory CO_2 release— and thus possible higher rates of simulated NPP—at sites further away from the equator, compared with current model scenarios. As replacement of a fixed Q_{10} formulation with our GPM is likely to have

profound effects on estimates of global plant R and calculations of NPP, its adoption in ESMs will adjust projections of both contemporary and future carbon storage in vegetation. This includes estimates of PFT composition in TBMs that also calculate biome extent through NPP-dependent competition rules. Furthermore, via influence on atmospheric CO_2 levels, the GPM will affect estimates of what constitutes "permissible" fossil fuel emissions needed to stay below any warming thresholds that society determines as unsafe to cross. This might include the presently much-debated limit of 2° warming since the preindustrial era (32, 33).

Finally, a priority for environmental science remains the building and operating of ESMs with robust parameterizations, allowing trustworthy forward projections of carbon cycle evolution and assessment of the influence of fossil fuel burning on that cycle and associated implications for future climate change. Plant respiration, and any adjustment to that in response to global warming, places a strong control on earth's carbon cycle and may modulate human influence on future atmospheric CO_2 concentrations. The urgency to estimate climate change implies ESMs must be operated routinely, both now and in the future. Computational constraints, combined with limited available data, force a compromise in ESMs where numerical code "lumps" features of terrestrial ecosystems into low numbers of PFTs and relatively general parameterizations. Our study across a massive dataset of leaf R measurements, and subsequent testing and fitting to a model of T response, shows a remarkable level of invariance between geographical sites and biomes. This provides great encouragement that, for leaf R at least, the generality of ESMs can be viewed as a neutral, or perhaps, positive feature.

Methods

Field Sites and Species. Details on the 18 field sites used in our study are provided in *Supporting Information* and Table S1, and a full list of all 231 species included in this study can be found, grouped by site and biome, in Dataset S1.

High-Resolution Measurements of the Temperature Response of Leaf Respiration. At each field site, replicate branches of sunlit leaves were used to generate high-resolution R–T curves (see *Supporting Information* for details). In brief, whole replicate leaves from these branches, or shoot segments for conifers and small-leaved species, were placed in a T-controlled, well-mixed cuvette, and allowed to adapt to darkness for 30 min. Leaf cuvettes were T controlled via a thermostatically controlled circulating water bath as in O'Sullivan et al. (27) and Heskel et al. (34), or via a Peltier system (3010-GWK1 Gas-Exchange Chamber; Walz, Heinz Walz GmbH). After the 30-min dark adaption period, the cuvette chamber was cooled to 10 °C. Thereafter, the cuvette chamber was heated continuously at a rate of 1 °C min^{-1} until a maximum rate of respiration was reached (generally leaf T between 55 and 70 °C), although only data up to $T = 45$ °C was used in our model. The net release of CO_2 from leaves was recorded at 30-s intervals. Postmeasurement, each replicate leaf was removed from the cuvette, placed in a drying oven at ~60 °C for a minimum of 2 d, and weighed afterward, so that rates could be expressed on a dry-mass basis (nmol CO_2 g^{-1} s^{-1}).

Quantification of R–T curves and Model Comparison. The 673 R–T curves collected by the methods described above required thorough quantification for comparison across replicates, species, sites, biomes, and plant functional types. For each replicate R–T response curves, we assessed the fits commonly applied R–T models, including: (*i*) an exponential model with a fixed-Q_{10} across the entire T range (though not specifically a fixed Q_{10} of 2, as is applied in some biosphere models of R); (*ii*) an Arrhenius model; (*iii*) a model of R responding to the UTD as defined by Gillooly et al. (15), which contains an activation energy parameter and uses Boltzmann's constant; (*iv*) a model presented by Lloyd and Taylor (17) to describe the response of soil R to T that includes a temperature-sensitive activation energy; (*v*) a model that incorporates a variable-Q_{10} response across the T range as described by two parameters; and (*vi*) a simple second-order polynomial model. Equations for these models are shown in *Supporting Information*. To compare how these models fit to data, we fitted each of the aforementioned models to all replicate R–T response curves in JMP (Version 11; SAS Institute), with parameters calculation controlled by the minimal residuals produced from each individual fit for each model. In cases where model convergence was not possible via the curve-fitting software, those replicate curves were not included to calculate mean residuals for the model fit over all replicates. Further, to evaluate the impact of different measurement

temperature span (i.e., 10–45 °C vs. 20–45 °C) on model fits, we compared fit coefficients across all replicate curves at different segmented intervals of the response curve (Table S2, Fig. S3, and *Supporting Information*). Using these data, we also compared model fit coefficients from the approximate 20 °C *T* range that best represents the climate of that species (the "ecologically relevant" *T* range; Table S3 and *Supporting Information*) to the fit coefficients calculated from all available data from the entire measurement *T* range.

Global Polynomial Model Calculation. After polynomial curve fit analysis, each replicate curve could be defined by specific *a, b,* and *c* parameters. The mean value of replicates for individual species at given sites were calculated for *a, b,* and *c,* resulting in a total of 231 species-site means of these parameters used for our study. To create a "global model" of the *T* response of *R,* we calculated the mean of all 231 species-site mean values of the *a, b,* and *c* parameters.

Modeling Site-Based Leaf *R* with JULES. For our 18 field sites, we incorporated our derived global *T* response (Eq. 3), with local values of R_{Tref}, into an offline version of Joint U.K. Land Environmental Simulator (JULES) to investigate the potential impacts of altered *T* sensitivity of *R*. JULES is the land-surface model of the U.K. Hadley Centre HadGEM (Hadley Centre Global Environment Model) family of global circulation models (28, 35). In its current form, JULES assumes that leaf *R* doubles for every 10 °C rise in *T* (i.e., $Q_{10} = 2$); other TBM frameworks have also assumed fixed Q_{10} [e.g., BIOME-BGC (36), PnET-CN (37) CLM4 (38), TEM (39)], or modified Q_{10} [e.g., BETHY (40)] functions. This is done using both the fixed Q_{10} and GPM formulations, and with JULES adopting the site-mean values leaf *R* at $R_{Tref} = 25$ °C derived from our short-term *T* response curves. The Q_{10} value is set as 2.0 for all

18 sites, and similarly for the GPM model, the *b* and *c* parameters are invariant, taking their cross-site means (Table 1 and Eq. 3).

Here we use a version of JULES driven with the WATCH (water and global change) Forcing Data ERA-interim (WFDEI) surface climatology (41) for each of the 18 sites and for the period 2010–2014 inclusive. Each site uses the WFDEI gridded data values from its 0.5′ × 0.5′ grid resolution nearest to site location; and in time is therefore a subset of the WFDEI data, presently covering 1979–2014. The DGVM (Dynamic Global Vegetation Model) component of JULES is kept switched off, and therefore known local values of leaf area index (LAI) are prescribed. Four JULES PFTs were adopted (broadleaf trees, needleleaf trees, shrubs, and C_3 grasses/herbs). With the DGVM off, then the main difference between these PFTs is the inclusion of deciduous phenology (where observed, affecting the prescribed LAI), and slightly different response curves for stomatal opening.

Our runs are made for each site, weighed by known fractional covers of the four PFTs above (predominantly broadleaf trees). The actual JULES model diagnostic presented (Fig. 3) is the canopy-top-level *R* value [μmol CO_2 (m^{-2} of leaf cover)$^{-1}$ s^{-1}), representing those fluxes that might be observed in fully sun-exposed leaves at the canopy crown, if fluxes from lower leaves were ignored.

1. Canadell JG, et al. (2007) Contributions to accelerating atmospheric CO_2 growth from economic activity, carbon intensity, and efficiency of natural sinks. *Proc Natl Acad Sci USA* 104(47):18866–18870.
2. IPCC (2013) *Climate Change 2013: The Physical Science Basis. Contribution of Working Group I to the Fifth Assessment Report of the Intergovernmental Panel on Climate Change*, eds Stocker TF, et al. (Cambridge University Press, Cambridge, UK).
3. Atkin OK, Scheurwater I, Pons TL (2007) Respiration as a percentage of daily photosynthesis in whole plants is homeostatic at moderate, but not high, growth temperatures. *New Phytol* 174(2):367–380.
4. Amthor JS (2000) The McCree-de Wit-Penning de Vries-Thornley respiration paradigms: 30 years later. *Ann Bot (Lond)* 86(1):1–20.
5. Atkin OK, Tjoelker MG (2003) Thermal acclimation and the dynamic response of plant respiration to temperature. *Trends Plant Sci* 8(7):343–351.
6. King AW, Gunderson CA, Post WM, Weston DJ, Wullschleger SD (2006) Atmosphere. plant respiration in a warmer world. *Science* 312(5773):536–537.
7. Valentini R, et al. (2000) Respiration as the main determinant of carbon balance in European forests. *Nature* 404(6780):861–865.
8. Huntingford C, et al. (2013) Simulated resilience of tropical rainforests to CO2-induced climate change. *Nat Geosci* 6(4):268–273.
9. Pappas C, Fatichi S, Leuzinger S, Wolf A, Burlando P (2013) Sensitivity analysis of a process-based ecosystem model: Pinpointing parameterization and structural issues. *J Geophys Res Biogeosci* 118(2):505–528.
10. Booth BBB, et al. (2012) High sensitivity of future global warming to land carbon cycle processes. *Environ Res Lett* 7(2):024002.
11. Atkin OK, Meir P, Turnbull MH (2014) Improving representation of leaf respiration in large-scale predictive climate-vegetation models. *New Phytol* 202(3):743–748.
12. Atkin OK, Bruhn D, Tjoelker MG (2005) *Response of Plant Respiration to Changes in Temperature: Mechanisms and Consequences of Variations in Q_{10}; Values and Acclimation. Plant Respiration, Advances in Photosynthesis and Respiration*, eds Lambers H, Ribas-Carbo M (Springer, Dordrecht, The Netherlands), Vol 18, pp 95–135.
13. Blackman FF, Matthaei GL (1905) Experimental researches in vegetable assimilation and respiration. IV.–A quantitative study of carbon-dioxide assimilation and leaf-temperature in natural illumination. *Proc R Soc Lond B* 76(511):402–460.
14. Wager HG (1941) On the respiration and carbon assimilation rates of some arctic plants as related to temperature. *New Phytol* 40(1):1–19.
15. Gillooly JF, Brown JH, West GB, Savage VM, Charnov EL (2001) Effects of size and temperature on metabolic rate. *Science* 293(5538):2248–2251.
16. Tjoelker MG, Oleksyn J, Reich PB (2001) Modelling respiration of vegetation: Evidence for a general temperature-dependent Q10. *Glob Change Biol* 7(2):223–230.
17. Lloyd J, Taylor JA (1994) On the temperature dependence of soil respiration. *Funct Ecol* 8:315–323.
18. Amthor JS (1984) The role of maintenance respiration in plant growth. *Plant Cell Environ* 7(8):561–569.
19. Ryan MG (1991) Effects of climate change on plant respiration. *Ecol Appl* 1(2):157–167.
20. James WO (1953) *Plant Respiration* (Clarendon Press, Oxford).
21. Mahecha MD, et al. (2010) Global convergence in the temperature sensitivity of respiration at ecosystem level. *Science* 329(5993):838–840.
22. Zaragoza-Castells J, et al. (2008) Climate-dependent variations in leaf respiration in a dry-land, low productivity Mediterranean forest: The importance of acclimation in both high-light and shaded habitats. *Funct Ecol* 22(1):172–184.
23. Atkin OK, et al. (2015) Global variability in leaf respiration in relation to climate, plant functional types and leaf traits. *New Phytol* 206(2):614–636.
24. Vanderwel MC, et al. (2015) Global convergence in leaf respiration from estimates of thermal acclimation across time and space. *New Phytol* 207(4):1026–1037.
25. Slot M, Kitajima K (2015) General patterns of acclimation of leaf respiration to elevated temperatures across biomes and plant types. *Oecologia* 177(3):885–900.
26. Wythers KR, Reich PB, Bradford JB (2013) Incorporating temperature-sensitive Q_{10} and foliar respiration acclimation algorithms modifies modeled ecosystem responses to global change. *J Geophys Res Biogeosci* 118(1):77–90.
27. O'Sullivan OS, et al. (2013) High-resolution temperature responses of leaf respiration in snow gum (*Eucalyptus pauciflora*) reveal high-temperature limits to respiratory function. *Plant Cell Environ* 36(7):1268–1284.
28. Clark DB, et al. (2011) The Joint UK Land Environment Simulator (JULES), model description - Part 2: Carbon fluxes and vegetation dynamics. *Geosci Mod Dev* 4(3):701–722.
29. Reich PB, et al. (2008) Scaling of respiration to nitrogen in leaves, stems and roots of higher land plants. *Ecol Lett* 11(8):793–801.
30. Reich PB, et al. (1998) Relationships of leaf dark respiration to leaf nitrogen, specific leaf area and leaf life-span: A test across biomes and functional groups. *Oecol* 114(4):471–482.
31. Smith NG, Dukes JS (2013) Plant respiration and photosynthesis in global-scale models: Incorporating acclimation to temperature and CO2. *Glob Change Biol* 19(1):45–63.
32. Huntingford C, et al. (2012) The link between a global 2 °C warming threshold and emissions in years 2020, 2050 and beyond. *Environ Res Lett* 7:014039.
33. Rogelj J, et al. (2011) Emission pathways consistent with a 2°C global temperature limit. *Nat Clim Chang* 1(8):413–418.
34. Heskel MA, et al. (2014) Thermal acclimation of shoot respiration in an Arctic woody plant species subjected to 22 years of warming and altered nutrient supply. *Glob Change Biol* 20(8):2618–2630.
35. Best MJ, et al. (2011) The Joint UK Land Environment Simulator (JULES), model description - Part 1: Energy and water fluxes. *Geoscic Mod Dev* 4(3):677–699.
36. Wang W, et al. (2009) A hierarchical analysis of terrestrial ecosystem model Biome-BGC: Equilibrium analysis and model calibration. *Ecol Modell* 220:2009–2023.
37. Ollinger SV, Aber JD, Reich PB, Freuder RJ (2002) Interactive effects of nitrogen deposition, tropospheric ozone, elevated CO_2 and land use history on the carbon dynamics of northern hardwood forests. *Glob Change Biol* 8(6):545–562.
38. Bonan GB, et al. (2011) Improving canopy processes in the Community Land Model version 4 (CLM4) using global flux fields empirically inferred from FLUXNET data. *J Geophys Res Biogeosci* 116(G2):G02014.
39. Melillo JM, et al. (1993) Global climate change and terrestrial net primary production. *Nature* 363(6426):234–240.
40. Ziehn T, Kattge J, Knorr W, Scholze M (2011) Improving the predictability of global CO_2 assimilation rates under climate change. *Geophys Res Lett* 38(10):L10404.
41. Weedon GP, et al. (2014) The WFDEI meteorological forcing data set: WATCH forcing data methodology applied to ERA-Interim reanalysis data. *Water Resour Res* 50(9):7505–7514.
42. Cox PM, Betts RA, Jones CD, Spall SA, Totterdell IJ (2000) Acceleration of global warming due to carbon-cycle feedbacks in a coupled climate model. *Nature* 408(6809):184–187.
43. Cox P (2001) *Description of the "TRIFFID" Dynamic Global Vegetation Model* (Hadley Centre, Met Office, Bracknell, UK), pp 1–16.
44. Huntingford C, Cox PM, Lenton TM (2000) Contrasting responses of a simple terrestrial ecosystem model to global change. *Ecol Modell* 134:41–58.
45. Monteith JL (1981) Evaporation and surface temperature. *Q J R Meteorol Soc* 107(451):1–27.
46. Hijmans RJ, Cameron SE, Parra JL, Jones PG, Jarvis A (2005) Very high resolution interpolated climate surfaces for global land areas. *Intern J Clim* 25:1965–1978.

ECOLOGY